

908699

TIRE WEAR MODEL

Edward Saibel and Chenglong Tsai

Dept. of Mechanical Engineering  
Carnegie-Mellon University  
Pittsburgh, Pa. 15213

November 1969

Interim Report No. 2 for Period August 15 to November 15, 1969

Prepared for

Tire Systems Section  
Office of Vehicle Systems Research  
NATIONAL BUREAU OF STANDARDS  
Washington, D. C. 20234

CST-854-5

This report was prepared under National Bureau of Standards Contract CST-854-5 (funded by the Air Force Flight Dynamics Laboratory, Delivery Order No. F33615-69-M-5011/Project No. 1369/Task No. 136903). The opinion, findings, and conclusions expressed in this publication are those of the authors and not necessarily those of the National Bureau of Standards nor the AF Flight Dynamics Laboratory.

Reproduced by the  
CLEARINGHOUSE  
for Federal Scientific & Technical  
Information Springfield Va. 22151

Best Available Copy

## Table of Contents

- I. Introduction
  - II. Tire Wear Formulas (for automobile)
    1. How the formulas were derived
    2. What can be inferred from the formulas
    3. Factors that affect wear rate
  - III. Fatigue Failure of Rubbers
    1. Fatigue curve (Wöhler Curve)
    2. The tearing energy criterion
  - IV. Activation Energy and Wear
    1. Thermo-activation equation for abrasion
    2. Temperature effect
  - V. Frictional Temperature Rise of Tires
    1. Viehmann's derivations
    2. Schallamach's derivations
  - VI. Thermodynamics and Rubber Deformation
    1. Fundamental principles
    2. Experimental investigations
    3. The thermo-elastic inversion phenomenon
    4. Thermal effects of extension
  - VII. Energy Balance for Wear Process
  - VIII. Influence of the Type of Stress on the Failure of Rubbers and Elastomers
- References
- Tables
- Figures
- Best Available Copy

## I. Introduction

Tire wear depends on many factors. Some of these factors are mentioned in a previous report [1]\*. A careful study of these factors reveals that a single tire wear formula can not describe the complicated phenomenon suitably. We will go into this in more detail below.

In general, different tread materials are differently affected by those factors which affect wear rate. Conventionally determined road wear ratings usually do not allow detailed conclusions to be drawn with respect to the relative importance of the factors as they refer to tire wear under ordinary conditions. Another problem is that factors influencing road wear may not be independent of each other.

In this report we compare wear formulas in the literature, we examine the fatigue phenomenon, and the temperature effect on wear rate. Finally we will look into rubber deformation as related to basic thermodynamic concepts and examine the feasibility of an energy balance approach for the wear process.

## II. Tire Wear Formulas (for automobile tires)

The following formulas have received wide attention

$$A = \sigma^2 P f r_0 [1 + \alpha(t_s - t_0) + c d] \quad (1)$$

$$A = \text{const.} (E/\sigma_0) \mu^{\delta - \beta\delta - 1} (\sigma a)^{2 + \beta\delta} / (2 + \beta\delta) \quad (2)$$

$$A = K (P \sigma^2 + Q \sigma^{3.5}) \quad (3)$$

\*Numbers in the brackets refer to references.

Here  $\Lambda$  = wear rate

$\theta$  = slip angle

$\rho$  = resilience of the wheel

$f$  = wheel stiffness

$\gamma_0$  = abradability

$\alpha$  = temperature coefficient

$t_s$  = tire surface temperature

$t_0$  = reference temperature at which  $\gamma = \gamma_0$

$c$  = constant

$d$  = spacing of abrasion pattern

$E$  = modulus of elasticity

$\sigma_0$  = ordinary tensile strength

$\mu$  = coefficient of friction

$\delta$  = fatigue exponent

$\beta$  = parameter specifying track roughness

$a$  = length of contact area

$K$  = constant

$P$  = material constant

$C$  = material constant

1.) Their origins are as follows

Schallamach [2, 3] starting from the abrasion of an ideally elastic wheel with an elliptic pressure distribution over the area of contact, derived a wear formula for slipping wheels. In this formula he found that wear rate was not consistent with what was to be expected. Then he modified it by considering the effect of an abrasion pattern and a temperature effect, finally arriving at equation (1).

Kraghelsky and Nepomnyashchi [4] based on a fatigue theory and the geometry of the contact surface derived the wear formula for wheels rolling with slip as in equation (2).

Bulgin and Walters [5] made experiments with large varieties of different rubber materials. They found that different materials have different wear mechanisms which introduced deviations when equations (1) and (2) were used to describe wear rate. Using a combination of abrasive and fatigue wear they set up an empirical relation for tire wear as given by equation (3).

## 2.) What can be inferred from the formulas

Apparently equation (1) shows the importance of the slip angle and the tire surface temperature. The properties of the wheel are included. The properties of the contact surface are implicitly expressed by the abradability term. But according to Bulgin and Walter's data [5], a high styrene SBR (Styrene-butadiene rubber) has a negative temperature coefficient. This seems unreasonable.

In equation (2) the tangential load (longitudinal and lateral force or side slip angle), length of the contact area, roughness, elasticity and strength properties are involved. The dependence of slip angle on wear has a power of  $(2+\beta\delta)$  which is approximately 2.43. This is the special characteristic of fatigue wear which distinguishes itself from abrasive wear which usually has a power of 2. Temperature effect is not included in equation (2).

Equation (3) has the advantage of taking care of the change of slip angle dependence, but it can not give any information other than

slip angle. Fig. 7 shows some results from [5] which fit equation (3) well.

Reviewing the deficiencies stated above and realizing the different properties for different kinds of rubber one can easily see the difficulty in setting up a unified equation to describe the tire wear phenomenon.

3.) Factors that effect wear rate

Kraghelsky and Nepomnyashchi [6] from a fatigue mechanism demonstrated some of the effects of basic factors on wear. Fig. 1 shows how wear depends on pressure, slip, the coefficient of friction, the roughness of the surface, the elastic modulus, the strength and the resistance of the rubber to fatigue. It should be noted, however, that these relationships are idealized, since these parameters are interconnected. For example, pressure influences both slip (slip decreases with increase in pressure) and coefficient of friction; the stress, strength and fatigue properties are also interconnected. Hence, during experimental determinations of these relationships it is essential to select the samples and test conditions extremely carefully, so that when one parameter is changed the others change as little as possible.

Bulgin and Walters [5] studied the wear rate on asperity surfaces and smooth textured surfaces (which Schallsmach called "sharp abrasives" and "blunt abrasives"). In general, on asperities the wear rate is proportional to applied load, modulus of elasticity, carbon content, temperature and the sliding distance. On the smooth surfaces wear rate is proportional to the power of applied stress, while the carbon content and temperature have an inverse effect. However, we should notice that

there are many exceptions as will be seen from the following figures. Fig. 2 gives the temperature effect on asperity surfaces for different kinds of rubbers. Fig. 3 gives the case for smooth surfaces. As seen from the figure, the proportionality between wear and those factors affecting wear rate may only be true in a certain regime.

### III. Fatigue failure of Rubbers

When a tire rolls on the road surface it is easy to see the tire surface is subject to a cyclic action of extension and compression. Due to this cyclic action on the tire surface, fatigue of rubber will occur after a certain number of cycles is performed, i.e. fracture cracks and their propagation will occur. There are several different approaches in investigating this phenomenon, two of which will be discussed below.

#### 1.) Fatigue curve (Wöhler curve)

Reznikovskii [7] investigated fatigue wear and proposed an empirical relation to describe the fatigue life of rubber

$$n = \left( \frac{\sigma_0}{\sigma} \right)^\delta$$

(4)

where  $n$  = the number of cycles to failure

$\sigma$  = amplitude of the stress

$\sigma_0$  = constant with the physical meaning of the breaking stress when

$n = 1$ ; and

$\delta$  = a constant expressing the resistance of the material to repeated loading.

Later Kraghelsky et al. [8] checked the applicability of this relation experimentally and established a relationship between normal (volume) fatigue phenomena and contact (surface) fatigue. They found that there is no significant difference between the two for some materials. It is obvious that in the abrasion of rubber by a fatigue mechanism, we are interested in contact fatigue (caused by tangential force).

When slipping occurs, both compression zone and elongation zone are formed, whereas the elongation is most dangerous from the point of view of possible failure. According to present solutions of contact problems in elasticity theory [9, 10] the maximum stress in the elongation zone is proportional to the product of the maximum contact pressure and the coefficient of friction. Therefore, a first approximation would be:

$$\sigma_{red} = K f P_r = K \tau \quad (5)$$

where  $\sigma_{red}$  = the stress, reduced to simple elongation

$P_r$  = the mean actual pressure

$\sigma_H$  = the maximum contact pressure

$K$  = coefficient of proportionality

$f$  = coefficient of friction

$\tau$  = the shear stress

Fig. 4 shows fatigue curves, determined experimentally, for an unfilled natural rubber vulcanizate. The results given confirm the

applicability of equations (4) and (5) and show that the value of  $\delta$  (the slope of the fatigue curves in logarithmic coordinates), which expresses the ability of a material to resist repeated loading, is almost identical for volume and contact fatigue. Fig. 5 and 6 give fatigue curves for tread vulcanizates based on natural rubber and SKB (sodium-catalysed polybutadiene rubber) and on Europrene.

Comparison of volume fatigue curves with friction-contact fatigue curves gives reason to suppose that the breaking stress in the latter case is the elongation stress of the surface layer due to the friction force. The results obtained confirm the existence of a correlation between abrasion resistance and fatigue life of vulcanizates.

## 2.) The tearing energy criterion

Some types of test pieces (fig. 8) were used in determining the tearing energy and the fatigue life of rubbers [11]. A cut, generally about  $\frac{1}{2}$  mm long, is inserted in one edge and the test piece is repeatedly cycled to a fixed maximum extension, the minimum normally being zero. Measurements of the cut length  $c$  at suitable intervals of  $n$  cycles enable the cut growth rate  $dc/dn$  to be determined. For the tensile strip test piece [11]

$$T = 2kWc \quad (6)$$

where  $W$  is the strain energy density in the bulk test piece and  $k$  is a slowly varying function of strain which has been determined experimentally [12].

The cut growth rate  $dc/dn$  is primarily determined by the maximum tearing energy attained during a cycle. The latter can be calculated from equation (5) using the value of  $2kW$  at the maximum strain and the measured cut length  $c$ . Results obtained in this way for a natural rubber gum vulcanizate are shown in fig. 9. It has been verified that if a given tearing energy is attained the amount of cut growth which occurs is independent of the test piece used (fig. 10).

Experiments [13] on the propagation of cuts have enabled the fatigue failure of rubber subjected to repeated simple extensions to be quantitatively understood as a crack-growth process which commences at small naturally occurring flaws. From these experiments two mechanisms of flow or cut growth have been identified. One is "mechanico-oxidative" cut growth due to primarily mechanical rupture which can be facilitated by the presence of oxygen; the other is ozone cut growth which is a corrosive type of process caused by chemical breaking of the polymer molecules by ozone. It is found that no mechanico-oxidative cut growth occurs below a critical value of the energy available for crack propagation. This critical energy is related to primary molecular-bond strengths and is approximately constant for all rubbers.

From its cut-growth characteristics, the fatigue life of a rubber can be accurately predicted over a wide range of deformations and for various atmospheric conditions. Corresponding to the critical energy, there is a mechanical fatigue limit (analogous to the fatigue limit observed for metals). Below the fatigue limit, flaws at first grow only slowly in the presence of ozone until the critical energy is reached,

when failure ensues fairly rapidly. At higher deformations the more rapid mechanico-oxidative cut growth starts immediately and fatigue lives are much more shorter (fig. 11).

#### IV. Activation Energy and Wear

The temperature dependence of the durability (at nominal stress  $\sigma = \text{const.}$ ) for solids and polymers is expressed by the equation

$$\tau = \tau_0 \exp\left\{\frac{U}{RT}\right\} \quad (7)$$

where  $\tau_0$  is a constant numerically similar to the period of thermal oscillation of the atoms;  $U$  is the activation energy for the process of failure;  $R$  is Boltzmann's constant;  $T$  is the absolute temperature.

The activation energy  $U$  depends, for many solids, on the state of stress  $\sigma$ , and decreases according to the formula

$$U = U_0 - \gamma \sigma \quad (8)$$

where  $U_0$  is the activation energy of the elementary failure process in the absence of stress and is similar in value to the sublimation energy for metals and to the energy of chemical bonds for polymers;  $\gamma$  is a coefficient which depends on the nature of the structure of the material. Substituting equation (8) into (7), the temperature-time dependence of the strength of rubber may be expressed by

$$\tau = \tau_0 \exp\left\{\frac{(U_0 - \gamma \sigma)}{RT}\right\} \quad (9)$$

This is the equation Zhurkov and Narzulaev [14] used in their kinetic theory of strength.

2.) Thermic-activation equation for abrasion

When applying equation (9) to abrasion the role of fatigue life is then taken by abrasion resistance, i.e. the time necessary to abrade a certain amount of material. It is more convenient, however, to use the rate of failure, i.e. the rate of wear  $I$  which is recorded directly by experiments. Thus for abrasion [15]

$$\begin{aligned} I &= I_0 \exp\left\{-\frac{(U_0 - \lambda' \mu p)}{RT}\right\} \\ &= I_0 \exp\left\{-\frac{(U_0 - \lambda p)}{RT}\right\} \end{aligned} \quad (10)$$

where  $\mu$  is the coefficient of friction;  $\mu p$  the force of friction and  $\lambda'$  has the same physical sense as  $\gamma$  in equation (9);  $I_0$  is analogous to  $1/\tau_0$ .

The activation barrier  $U_0$  in abrasion is reduced by  $\lambda' \mu p$ . But, since  $\mu$  changes only slightly in the region below the flow temperature ( $T_f$ ) with changes in  $p$  and  $T$ , then  $\mu \lambda' = \lambda$  can be considered as constant.

When determining the physical sense of  $I_0$  we note that  $\tau_0$  is the minimum fatigue life, depending neither on temperature nor load. Failure at such a high rate may occur when either  $T \rightarrow \infty$  or  $\sigma$  is so great that  $\gamma \sigma$  completely counterbalances  $U_0$ . In such critical conditions the time dependence or activation nature of the failure process is lost.

## 2.) Temperature effect

Fig. 12 shows the relationship between  $\log I$  and  $1/T$  for several loads. According to equation (10), these coordinates should produce a straight line, with a slope proportional to activation energy  $U$ , where

$$U = U_0 - \lambda p \quad (11)$$

In fact, the experimental points do lie on a straight line, but sometimes a "break" is observed in the line. The data were obtained with all test materials abraded by metal gauze [16].

As we can see from the figures, if temperature changes from  $30^\circ\text{C}$  to  $60^\circ\text{C}$ , the wear rate may change by a factor up to 50, very significant effect.

Fig. 13 shows the effect of temperature on the abrasion on gauze (fatigue wear) and on abrasive paper (abrasive wear).

All the findings stated above are based on the so called molecular-kinetic theory of failure, according to which abrasion is the failure of chemical bonds as a result of certain fluctuations in the thermal movements of molecules. When the tangential force is great enough to eliminate the barrier  $U_0$ , then each thermal movement results in abrasion.

If abrasion is studied from the point of view of macro-failure then, in general, abrasion is a fatigue process: [15, 17, 18] failure of the surface takes place after repeated deformation by projections of abradant.

Notice that in fig. 12 the slope of the lines decreases with increases in load.

## 7. Frictional Temperature Rise of Tires

### 1.) Viehmann's derivations

Viehmann [19] attempted to determine the frictional temperatures which may occur in tires under various conditions. It was based on phenomenological theories of heat conduction. The temperature rise was found to be localized in boundary layers of the order of  $10^{-2}$  cm. From the estimated values of the temperatures (see table 1), he concluded that the abrasion which occurs under normal driving conditions is purely mechanical. Only under extreme conditions, such as in very rapid acceleration, or in case of locked wheels - particularly at what we call "contact bridges" or surface elevations - may we expect high frictional temperatures, which lie far above the decomposition temperature of rubber.

### 2.) Schallamach's derivations

Schallamach [20] assumed tire and road are taken to be in ideal contact with each other, and the temperature rise of a surface element is calculated as if it were in the surface of a semi-infinite body. Further assumption is that heat flows only at right angles to the contact surface because the low thermal conductivity of rubber allows lateral heat flow to be neglected. The problem to be solved is thus reduced to an one-dimensional one.

Starting from a theory of linear heat conduction, in a semi-infinite body [21] and through some lengthy derivations he obtained a maximum frictional temperature rise  $\theta_m$  which occurs at the rear of the contact area of a slipping wheel:

$$\theta_m = 64 R \frac{K^{1/2}}{\pi^{3/2} \lambda} \frac{V \mu^2 L^2}{K b a^3} t^{1/2} \quad (12a)$$

$$= 8 R \frac{K^{1/2}}{\pi^{3/2} \lambda} \frac{V^{1/2} \mu^2 L^2}{b a^{1/2}} s \quad (12b)$$

$$R = (K_r^{1/2} / \lambda_r) / (K^{1/2} / \lambda + K_r^{1/2} / \lambda_r) \quad (13)$$

where  $K_r$  = thermal diffusivity of road

$\lambda_r$  = thermal conductivity of road

$K$  = thermal diffusivity of tire

$\lambda$  = thermal conductivity of tire

$V$  = circumferential velocity which for moderate slip, can  
equated with the travelling velocity

$\mu$  = coefficient of friction

$L$  = the load of the tire

$a$  = length of contact area

$b$  = width of contact area

$t$  = the total sliding time

$s$  = slip

In the derivations Schallamach did not give the numerical values for equation (12), however he gave an expression for  $\theta(z)/\theta_m$  (where  $Z$  is the co-ordinate at right angles to the contact surface).

$$\frac{\theta(z)}{\theta_m} = e^{-\frac{z^2}{4\kappa t}} - \pi^{-1/2} \frac{z}{2(\kappa t)^{1/2}} (1 - \operatorname{erf} \frac{z}{2(\kappa t)^{1/2}}) \left\{ 1 - \frac{c^2}{1+c^2} \frac{z^2}{4\kappa t} \right\} \quad (14)$$

where erf is the error function,  $c$  stands for

$$c = (\pi/8) K a^2 s / \mu L \quad (15)$$

The value of  $c$  is small enough at moderate slip for the term in square brackets to be replaced by unity [2]. The ratio  $\theta(z)/\theta_m$  depends then only on  $z/2(Kt)^{1/2}$  and is shown as a function of this quantity in Fig. 14. A typical figure for  $K$  for tread rubber is  $1.7 \times 10^{-3} \text{ cm}^2/\text{sec}$ ; the sliding time  $t$  is of the order of  $10^{-2}$  sec. at a travelling speed of 30 mph. With these numerical values, the depth  $z$  at which the temperature has dropped to 1 per cent of the surface temperature is about 0.15 mm. The heat into which the frictional energy has been converted is therefore confined to a very thin surface layer. This fact is consistent with that pointed out by Viehmann [19].

Brunner [22] has determined the temperature profiles across the thickness of the tread of a travelling tire by means of thermocouples embedded in and on the tire. The drawn-out curve in Fig. 15, taken from Brunner's paper, shows the temperature distribution in a natural rubber tire travelling at 80 km/h and exhibits a well defined maximum. Brunner's measurements do not cover the critical region near the outside surface where, in any case, no constant temperature distribution can be maintained because of the periodically occurring frictional temperature rise. The dotted part of the curve in fig. 15 indicates schematically the instantaneous frictional temperature according to Schallamach [20] when

superimposed on Brunner's curve. For clarity, the horizontal scale of this transient has been expanded about ten-fold.

## VI. Thermodynamics and Rubber Deformation

### 1.) Fundamental principles

The first law of thermodynamics provides us with a definition of internal energy, namely

$$dE = dQ + dW \quad (16)$$

This equation states that the increase in internal energy  $dE$  in any change taking place in a system is equal to the sum of the heat added to it,  $dQ$ , and the work performed on it,  $dW$ . The second law defines the entropy change  $dS$  in any reversible process by the relation

$$T dS = dQ \quad (17)$$

Define Helmholtz free energy  $A$  by the relation

$$A = E - TS \quad (18)$$

Treloar [23] used the fact that the change in Helmholtz free energy in an isothermal process is equal to the work done on the system by the external forces and that the tension is equal to the change in Helmholtz free energy per unit extension.

He then obtained the following expressions:

$$\left(\frac{\partial S}{\partial l}\right)_T = -\left(\frac{\partial f}{\partial T}\right)_l \quad (19)$$

$$\left(\frac{\partial E}{\partial l}\right)_T = f - T\left(\frac{\partial f}{\partial T}\right)_l \quad (20)$$

where  $f$  is the tensile force, and  $l$  is the length, measured in the direction of the force. Equation (19) gives the entropy change per unit extension in terms of a measurable quantity  $(\partial f/\partial T)_l$ , the temperature coefficient of tension at constant length. Equation (20) gives a relationship for the corresponding internal energy change. These two equations are of fundamental importance in rubber elasticity, since they provide a direct means of determining experimentally both the internal energy and entropy changes accompanying a deformation. The only experimental data which are necessary to provide for this purpose are a set of equilibrium values of the tension at constant length over a range of temperatures. If, for example, the curve  $cc'$  in fig. 16 represents the variation with temperature of the force at constant length, its slope at the point  $P$ , which is  $(\partial f/\partial T)_l$ , is by equation (19), equal to the entropy change per unit extension  $(\partial S/\partial l)_T$  when the rubber is extended isothermally at the temperature  $T$ . In a corresponding way, the intercept of the tangent to the curve at  $P$  on the vertical axis  $T=0$  (absolute zero), is  $f - T(\partial f/\partial T)_l$ , which by equation (20) is equal to the internal energy change per unit extension  $(\partial E/\partial l)_T$ .

The course of the internal energy and entropy changes accompanying

the deformation may thus be obtained by direct inspection of the stress-temperature curves. In particular, if these curves are linear (as in Meyer and Ferri's data, Fig. 17) both internal energy and entropy terms are independent of temperature. If, in addition, the stress-temperature relation is represented by a straight line passing through the origin, the internal energy term is zero. It follows that in this case the elastic force arises solely from the change in entropy.

## 2.) Experimental investigations

A typical curve, representing the behavior of a rubber vulcanized with 8% of sulphur, is illustrated in fig. 18. The stress is seen to be very nearly proportional to the absolute temperature over a range of about 120 degrees. It is therefore concluded that the elastic tension is due almost entirely to the entropy term, in agreement with the prediction of the kinetic theory of elasticity. At about 213°K the temperature coefficient of tension exhibits an abrupt reversal of sign. This corresponds to the transition to the glass-hard state, where the rubber loses its characteristic extensibility. The behavior then corresponds to that of an ordinary hard solid, with the internal energy term dominant.

Fig. 19 shows some other stress-temperature curves for the same material. The results confirm Meyer and Ferri's original conclusions in a general way. Calculation of the terms  $(\partial S/\partial l)T$  and  $(\partial E/\partial l)T$  from the curves in fig. 19, by means of equations (19) and (20), yielded the result shown in Fig. 20. It is evident from this figure that the form of the force-elongation curve is effectively due to the entropy term  $(\partial S/\partial l)T$ .

Except at small extensions ( $< 100$  per cent) the internal energy term accounts for not more than one-sixth of the observed tension for free-energy change. At low extensions, however, the internal energy changes are of the same order of magnitude as the entropy term, while the latter, instead of remaining negative (as required by the kinetic theory), changes sign at an extension corresponding to the thermo-elastic inversion point.

### 3.) The thermo-elastic inversion phenomenon

In fig. 19 one can observe that whilst above 10 per cent elongation the tension at constant length increases with rising temperature, at lower elongations the variation with temperature is in the opposite direction. Meyer and Ferri interpreted this thermo-elastic inversion phenomenon in terms of the expansion of volume of the rubber on heating. This expansion will clearly have the effect of tending to increase the length at constant stress, which is equivalent to reducing the tension at constant length. At very low stresses the reduction in tension by thermal expansion exceeds the increase of tension to be expected from the kinetic theory of elasticity; the thermo-elastic inversion point is the elongation at which these two effects exactly balance.

The fact that volume changes enter into the thermo-elastic phenomenon of rubber in no way limits the applicability of the fundamental equations (19) and (20) for the derivation of the internal energy and entropy changes on extension. These relations are purely phenomenological; they do not imply any particular mechanism. It is in the interpretation—not in the derivation—of the internal energy and entropy changes that physical or molecular concepts may usefully be introduced. In this

connexion, the explanation of the thermo-elastic inversion put forward by Meyer and Ferri is of the utmost significance since it points to the importance of hitherto neglected volume changes in the discussion of the thermodynamics of rubber elasticity.

#### 4.) Thermal effects of extension

It has been found that when rubber is stretched adiabatically its temperature will rise. Also it was noticed that a piece of rubber, extended by a constant load, contracted when the temperature was raised, which means that at constant length the tension increased with increasing temperature.

By the second law of thermodynamics, as represented by equation (17), the evolution of heat ( $-dQ$ ) in a reversible change gives a direct measure of the change of entropy in the process. If heat is evolved on the extension of any material, the entropy change is negative. Conversely, if heat is absorbed, the entropy change is positive. On account of the smallness of the heat effects in rubber, it is usual to measure the change of temperature in an adiabatic deformation rather than the heat evolved in an isothermal deformation. Under adiabatic conditions, by definition, the entropy change is zero, and the change in temperature is given by the relation (since  $\delta T = \delta Q/C_L$ )

$$\left(\frac{\partial T}{\partial l}\right)_S = -\left(\frac{1}{C_L}\right)\left(\frac{\partial Q}{\partial l}\right)_T \quad (21)$$

where  $C_L$  is the specific heat at constant length, and  $-(\partial Q/\partial l)_T$  is the isothermal heat of extension. Thus the temperature change in a quick

extension from the initial length  $l_0$  to the final length  $l$  is obtained by integration of (21) with respect to  $l$ . Thus

$$\Delta T = -\frac{T}{C_e} \int_{l_0}^l (\partial S / \partial l)_T dl \quad (22)$$

Fig. 21 is a curve given by Joule (1859), who used a thermocouple in contact with the rubber for this purpose. The curve shows an initial cooling followed by a rapidly rising heating effect as the extension was increased. Later on a slight difference between the effects on extension and on retraction respectively was found, due to the irreversible phenomenon of relaxation. The data given in fig. 21 are mean figures for extension and retraction.

At higher elongations the variations in the heat effect, like the variations in internal energy change, are more complex and depend noticeably on the type of rubber. Typical data for a vulcanized latex rubber are shown in fig. 22. Up to about 250 per cent extension the curve is reversible. Beyond this point the heating increases rather sharply and is no longer reversible, the cooling on retraction being greater than the heating on extension. However, some other materials have the opposite phenomenon.

## VII Energy Balance for Wear Process

Chenea and Roach [24], based on the removal of wear particles from material as a wear process, derived some equations for mass balance and energy balance. After assuming an isothermal and steady state, the

mechanical wear between identical materials can be expressed by

$$\frac{dh}{dt} = \frac{\frac{1}{2} f P V}{\frac{S}{l} + \rho E_p} \quad (23)$$

$$\frac{1}{l} = \left\{ \frac{a \int_0^{\infty} \left(\frac{m}{p}\right)^{\frac{2}{3}} p(m) dm}{\int_0^{\infty} \left(\frac{m}{p}\right) p(m) dm} \right\} \quad (24)$$

where  $h$  = total change in surface level

$t$  = time

$f$  = friction coefficient

$P$  = normal load

$V$  = sliding velocity

$S$  = surface energy per unit area of wear particles

$\rho$  = density

$E_p$  = internal energy per unit mass of wear particles

$a$  = shape factor for wear particles

$m$  = mass of the particle

$p$  = frequency function

From equation (23)  $dh/dt$  can be interpreted as wear rate. On the right hand side, normal load, sliding velocity, surface energy and internal energy are all involved. However, the wear of tires is mostly interpreted as the fatigue failure of rubber. Thus the application of "removal of wear particles" may not be suitable for the tire wear process. A further inadequacy is the isothermal assumption, since we know tire wear will never be an isothermal process as we saw in the section on frictional

temperature rise. Although the approach does not fit the tire wear process too well the idea of using the energy balance for a wear process may be a promising way of solving the problems.

Rabinowicz [28] has attempted to account for wear in metals as a fracture process by equating the energy necessary to form fresh surfaces found in the wear particles to the energy necessary to produce a fracture. Such calculations have not been particularly successful up to now and it seems that energy methods are better applied through chemical and mechanical activation processes.

#### VIII. Influence of the Type of Stress on the Failure of Rubbers and Elastomers

The most critical type of stressed state for elastomers in tension under which various types of failure may be observed; rupture, shear, or a combination of rupture and shear (fig. 23). A complicated failure is observed in the specimen when in some neighborhood small tears grow towards each other and then join by local shear.

Types of failure are frequently met with in elastomeric strips [25] which are used to make sealing rings where under great and prolonged compression there appear, due to fatigue, slight tears in the packing which are either at an angle of  $45^{\circ}$  to the direction of the compression (fig. 24) or parallel to the contacting surfaces (fig. 25), where the side of the deformed packing bulges most. The rectangular cross-section of the packing takes on the shape of a "barrel" (fig. 26), whereby in the points A and B under great compression a tension appears in the lateral direction. The greater the compression of the packing, the more the free side surfaces bulge. Along the line AB of that "barrel" a growth of small

tears takes place from the surface into the depth of the material [27].

It should be noted in conclusion that very little work has been done on the failure of polymers and glasses under complicated stress systems [26].

Best Available Copy

## REFERENCES

- [1] Saibel, E. A., Interim Report for period May 15 to August 15, 1969 to NBS, Washington, D. C.
- [2] Schallamach, A. and Turner, D. M., *Wear*, 3 (1960) p. 1-25
- [3] Grosch, K. A. and Schallamach, A., *Wear*, 4 (1961) p. 356-371
- [4] Kraghelsky, I. V. and Nepomnyashchi, E. F., *Wear*, 8 (1965) 303-319
- [5] Bulgin, D. and Walters, M. H., Fifth Intern. Rubber Tech. Conf., Brighton, 1967
- [6] Kraghelsky, I. V. and Nepomnyashchi, E. F., *Abrasion of Rubber*, Palmerton Publishing Co., Inc., New York, p. 3-13
- [7] Reznikovskii, M. M., *Soviet Rubber Tech.*, 1960, 19, No. 9, 32
- [8] Kraghelsky, I. V., Reznikovskii, M. M., Brodskii, G. I. and Nepomnyashchi, E. F., *Soviet Rubber Tech.*, 1965, 24, No. 9, 30
- [9] Severin, M. M., *Contact strength of materials*, 1946, 2, see reference [6]
- [10] Koval'skii, B. S., *Izv, Akad. Nauk SSSR, Otdel. Tekhn. Nauk*, 1942, No. 9
- [11] Rivlin, R. S. and Thomas, A. G., *J. of Polymer Sci.*, 10, (1953), 291-318
- [12] Greensmith, H. W., *J. of Appl. Polymer Sci.*, 7 (1963), 933-1002
- [13] Lake, G. J. and Lindley, P. B., *Conf. Proc., Physical Basis of Yield and Fracture*, Oxford, 176-186, 1966
- [14] Zhurkov, S. N. and Narzulaev, B. N., *Zh. Tekhn. Fiz.*, 1953, 23, No. 10, 1677
- [15] Ratner, S. B., Thesis to the Karpov Physico-technical Institute, 1964
- [16] Ratner, S. B., *Dokl. Akad. Nauk SSSR*, 1960, 135, No. 2, 294
- [17] Ratner, S. B., *Dokl. Akad. Nauk SSSR*, 1963, 150, No. 4, 848
- [18] Kraghelsky, I. V., *Friction and Wear*, 1962
- [19] Viehmann, W., *Rubber Chemistry and Tech.*, Vol. 31 (1958), p. 925-40
- [20] Schallamach, A., *J. of the IRI*, vol. 1, No. 1, 1967
- [21] Carslaw, H. S. and Jaeger, J. C., 1958, *Conduction of Heat in Solids*, Oxford

- [22] Brunner, W., 1938, Deutsch Kraftfahrtforschung, Heft 2
- [23] Treloar, L. R. G., The Physics of Rubber Elasticity, 1958, Oxford, Second Edition
- [24] Chenea, P. F. and Roach, A. E., Lubrication Engineering, March/April, 1956 p. 123
- [25] Bartenev, G. M., Khim, prom. No. 8, 15 (1955)
- [26] Haward, R. N., The strength of Plastics and Glass, New York, 1949
- [27] Bartenev, G. M. and Zuyer. Yu. S., Strength and Failure of Visco-Elastic Materials, 1969, Pergamon Press
- [28] Rabinowicz, E. and Foster, R. G., Trans. ASME Series D. Vol. 86, No. 2, 1964, p. 306-12

TABLE I  
 FRICTION TEMPERATURES FOR VARIOUS DRIVING  
 CONDITIONS AND ROAD MATERIALS

Friction temperature, °C

Friction surfaces..... Driving conditions	Friction temperature, °C			Friction temperature, °C			Localization in the boundary layer, cm
	Asphalt	Basalt Concrete	Iron	Asphalt	Basalt Concrete	Iron	
1. Normal motor vehicle tire, 100 km/hr, slippage = 3%	15	10	2	60	40	8	$6.5 \times 10^{-3}$
2. Curved road, 50 km/hr, slippage = 10%	35	25	3.5	140	100	15	$9 \times 10^{-3}$
3. Spinning tire, 10 cycles/sec. slippage = 50%	240	160	24	(1000)	(650)	100	$7 \times 10^{-3}$
4. Locked skidding tire, max. 120 km/hr	(1100)	(700)	100			(400)	

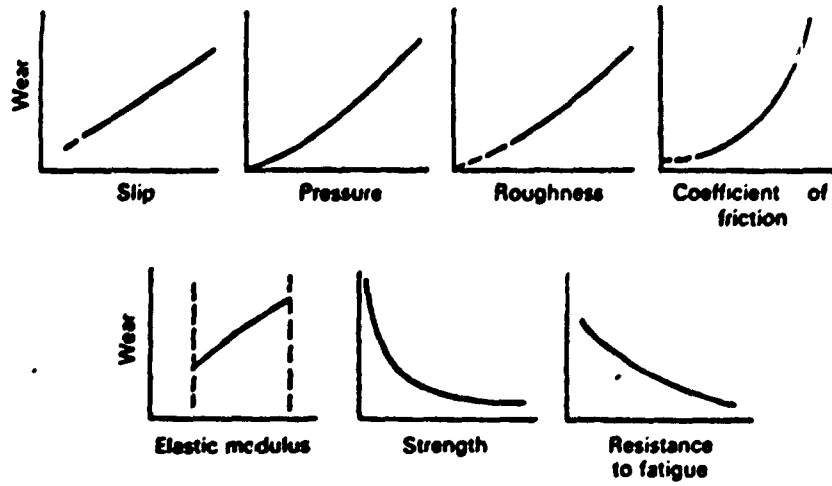


Fig. 1 The dependence of wear on the main parameters

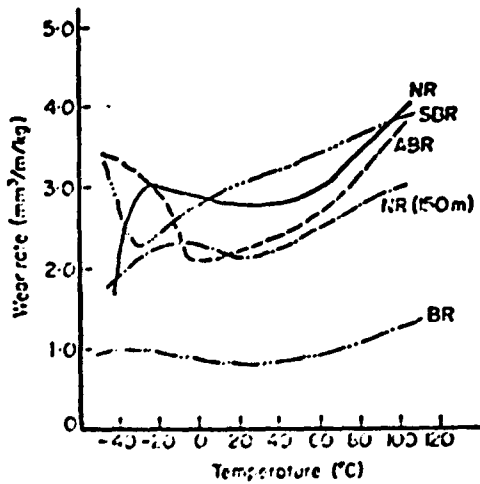


Fig. 2 Wear rate on asperities surfaces

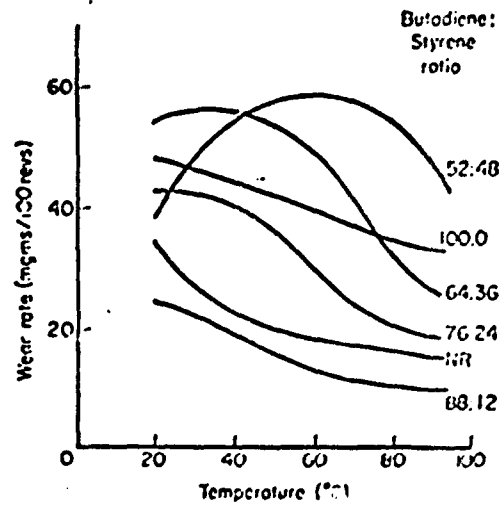


Fig. 3 Wear rate on smooth surfaces

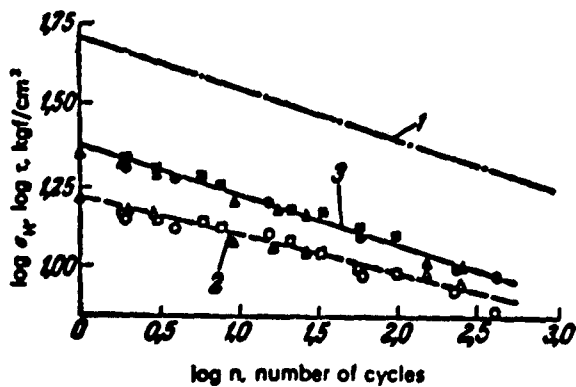


FIG. 4—Fatigue curves, obtained with the "PUPS" apparatus for an unfilled natural rubber vulcanizate: ○, ●—radius of curvature of indenter 2.0 mm; Δ, ▲—radius of curvature of indenter 1.5 mm; □, ■—radius of curvature of indenter 1 mm. 1—volume fatigue; 2—contact fatigue; 3—contact fatigue ( $\log \tau - \log n$ ).

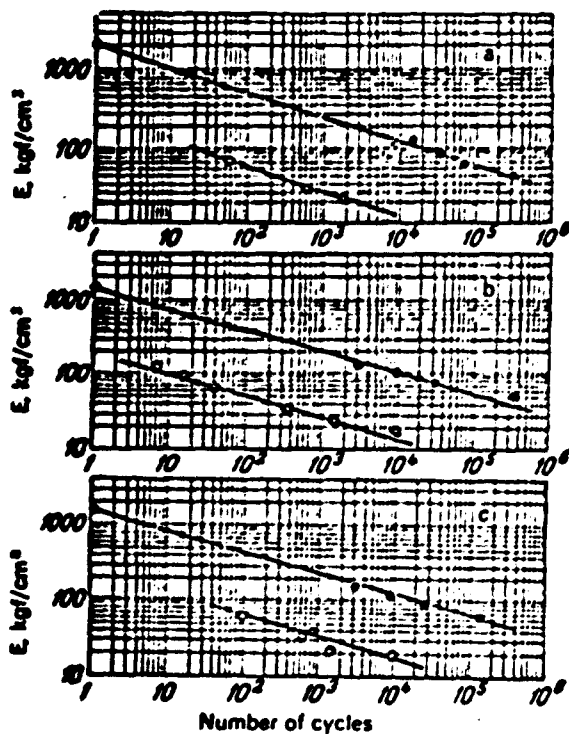


FIG. 5—Fatigue curves, obtained on the "Tsiklometr" apparatus, for Europrene tread vulcanizates: ●—repeated elongation; ○—contact fatigue ( $\log \tau - \log n$ ): a— $E = 22 \text{ kgf/cm}^2$ ; b— $E = 28 \text{ kgf/cm}^2$ ; c— $E = 32.5 \text{ kgf/cm}^2$ . (The ordinate axes should apparently be  $\sigma_n$ , or  $\tau$ ,  $E$  being the elastic modulus of the rubber; F.d.)

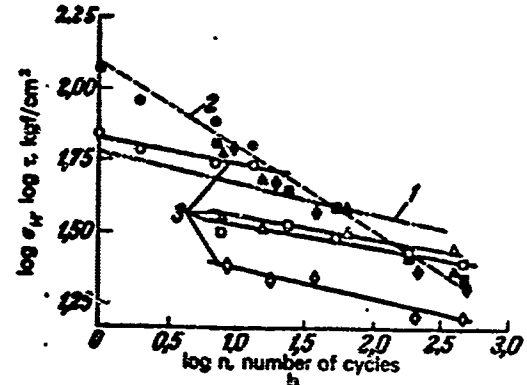
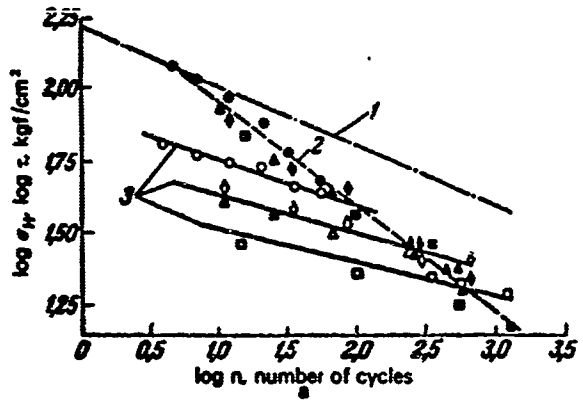


FIG. 6—Fatigue curves, obtained on the "PUPS" apparatus, for natural rubber (a) and SKB (b) tread vulcanizates: ●, ○—radius of curvature of indenter 0.5 mm; ▲, △—radius of curvature of indenter 1.0 mm; ■, □—radius of curvature of indenter 1.5 mm; ◊, ◇—radius of curvature of indenter 2.0 mm. 1—volume fatigue; 2—contact fatigue ( $\log \sigma_M - \log n$ ); 3—contact fatigue ( $\log \tau - \log n$ ).

- P Natural rubber/20 HAF
- Q Natural rubber/30 HAF
- R Natural rubber/50 HAF
- S Intcl 1500/50 HAF
- T Adiprene C/50 HAF
- U Polybutadiene/50 HAF

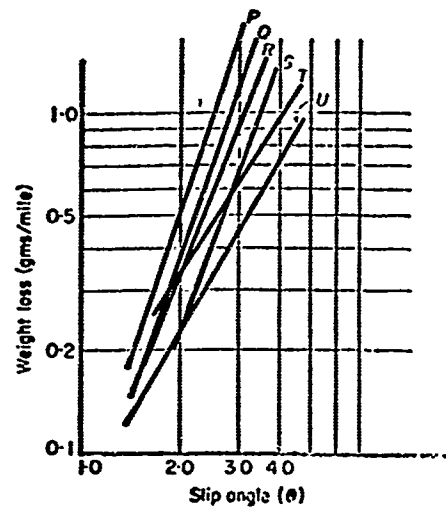


Figure 7 Logarithmic graphs of tyre abrasion against slip angle, showing that the wear rate increases as a power of the slip angle, varying from 1.8 to 3.2

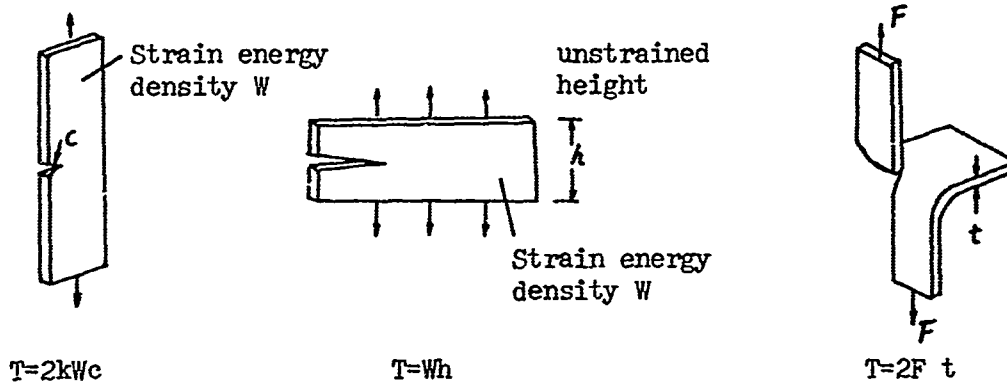


Figure 8. The tearing energy criterion. Various types of test piece which can be used for cut-growth measurements in rubber: left to right, tensile strip, pure shear and 'trousers' test pieces; the equations define the tearing energy for each test piece.

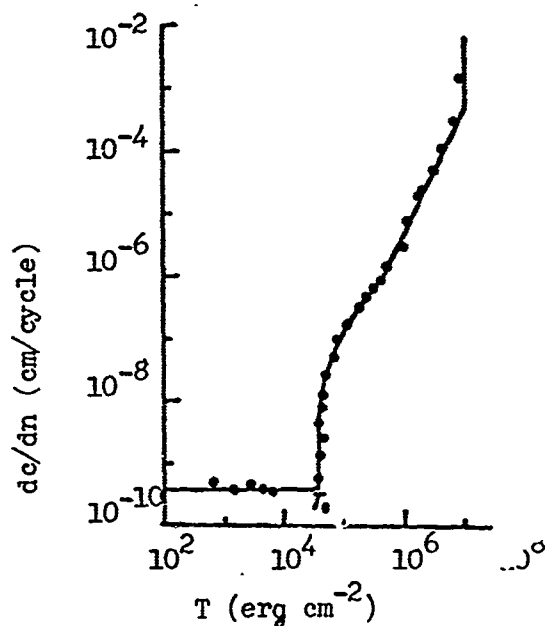
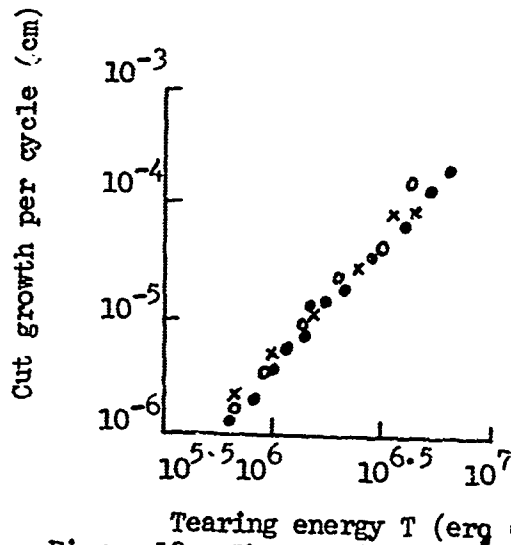


Figure 9. The relationship between cut growth and fatigue. Cut-growth results for natural rubber vulcanizate A obtained in the laboratory atmosphere at a frequency of 100 cycles/min (test pieces allowed to relax to zero strain on each cycle).



Tearing energy  $T$  ( $\text{erg cm}^{-2}$ )  
 Figure 10. The tearing energy criterion. Typical cut-growth results plotted against energy for the various types of test piece: ● tensile strip, X 'trousers', o pure shear.

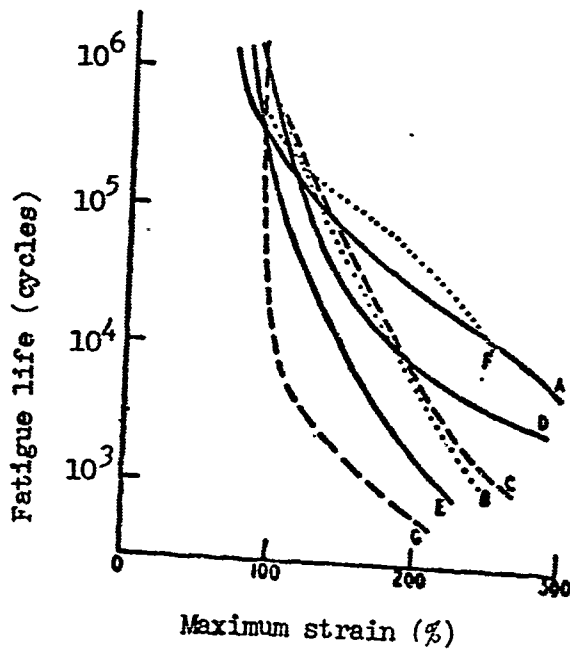


Figure 11. Fatigue behavior of various rubbers in the laboratory atmosphere (minimum strain zero): A, natural rubber (vulcanizate A); B, SBR (vulcanizate B); C, butyl rubber; D, polychloroprene; E, butadiene-acrylonitrile copolymer; F, synthetic cispolysoprene; G, polybutadiene. Rubbers A, D, F are strain crystallizing, C is weakly crystallizing, and B, E, G are non-crystallizing.

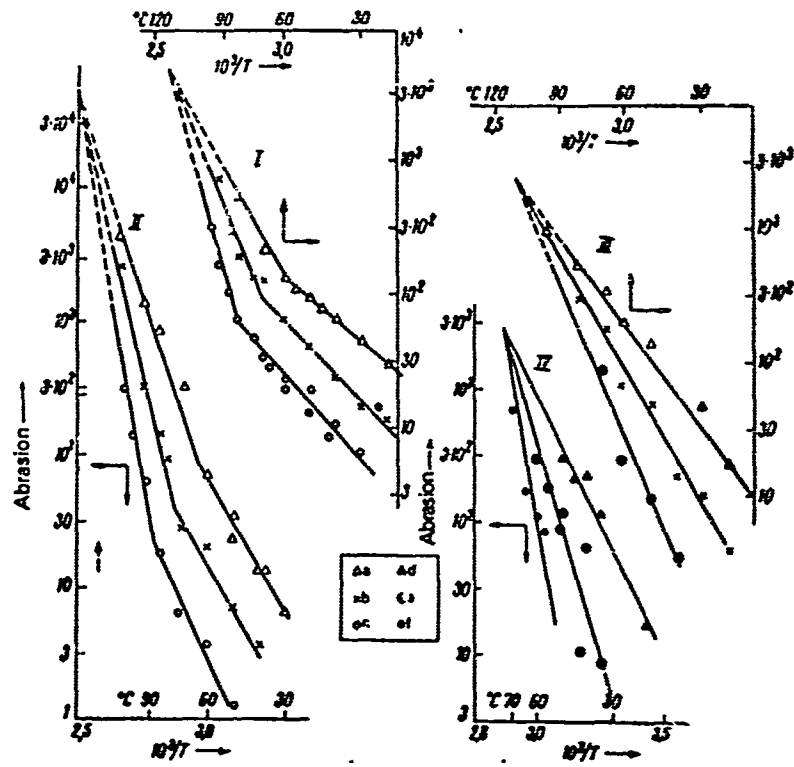


Fig. 12 Temperature dependence of abrasion on a gauze: I-h.p. polyethylene, II-PVC + 30% plasticizer; III-PVC + 80% plasticizer; IV-PMMA + 40% plasticizer. Load: a-2 kfg/cm<sup>2</sup>; b-1.3; c-0.65; d-0.3; e-0.15; f-0.06.

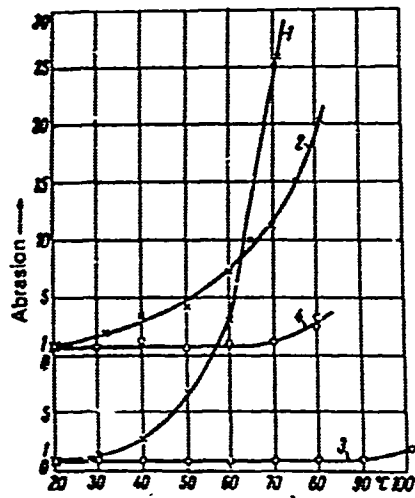


Fig. 13 Effect of temperature on the relative abrasion on a gauze (curves 1 and 2) and on abrasive paper (curves 3 and 4); 1 and 3-PVC; 2 and 4-h.p. polyethylene.

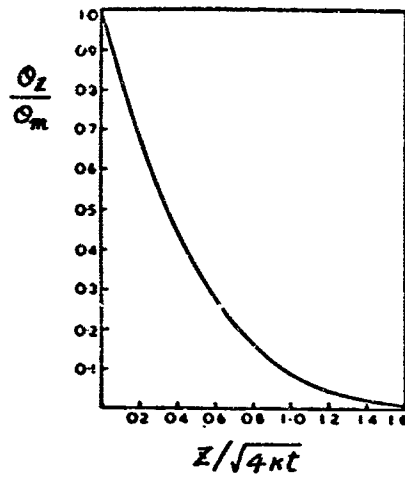


Fig. 14 The distribution of the frictional temperature rise below the surface of a slipping tyre

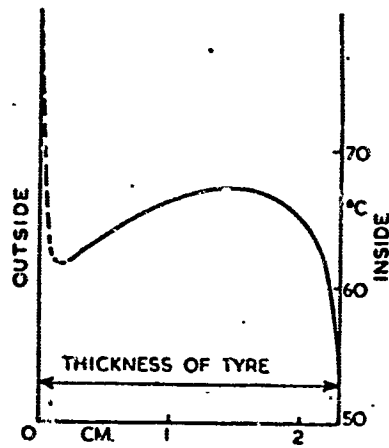


Fig. 15 Full curve: temperature distribution in a tyre after Brunner; interrupted curve: frictional temperature rise superimposed on Brunner's curve for an arbitrary slip

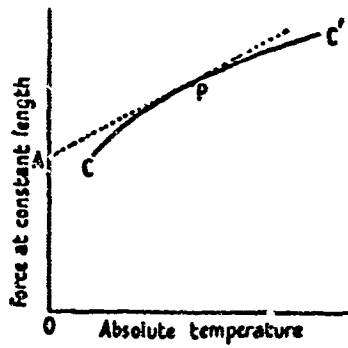


Fig. 16 Slope and intercept of stress-temperature curve

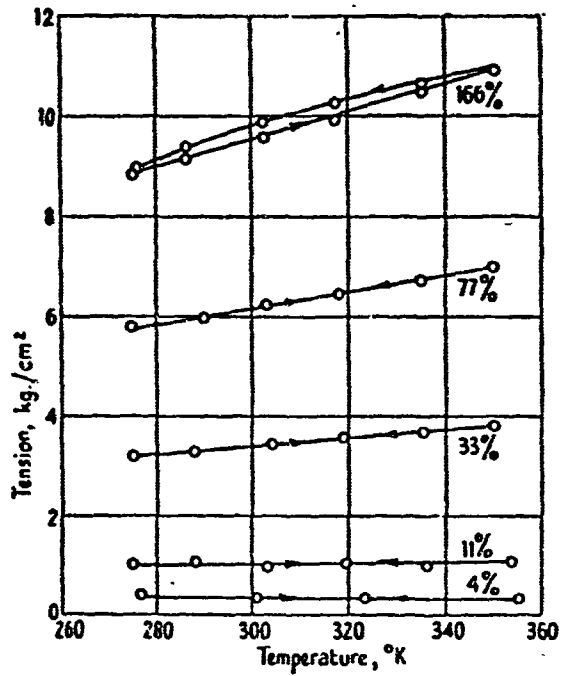


Fig. 17 Force at constant length as function of absolute temperature. Elongations as indicated. (Meyer and Ferri, 1935)

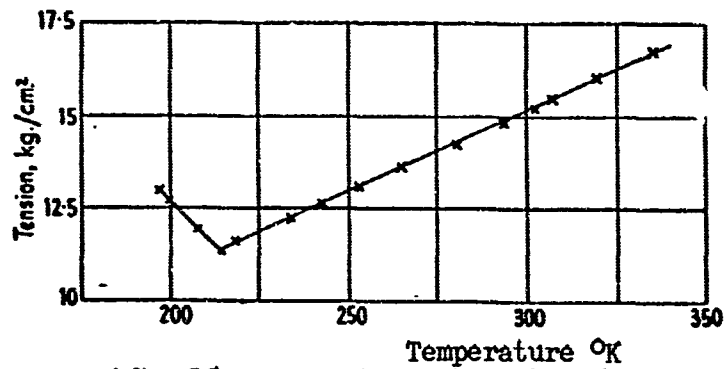


Fig. 18 Force at constant length as function of temperature. Elongations as indicated. (Anthony, Caston, and Guth, 1942)

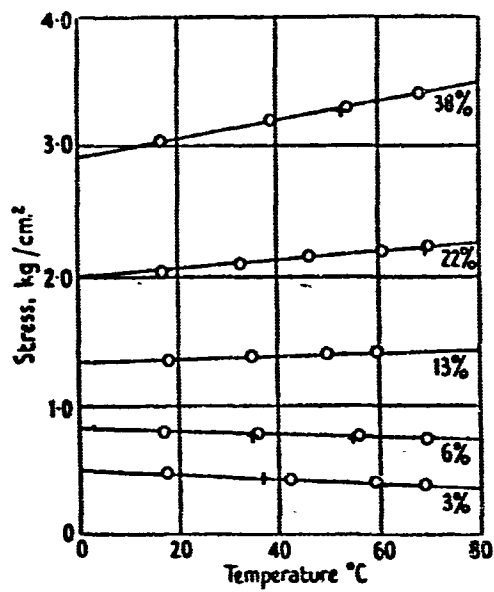


Fig. 19 Force at constant length as function of temperature. Elongations as indicated. (Anthony, Caston, and Guth, 1942)

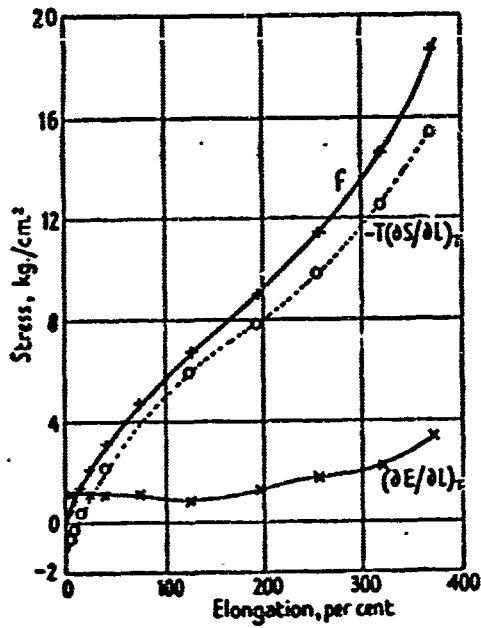


Fig. 20 Changes in internal energy (E) and entropy (S) accompanying extension of rubber. (Anthony, Caston and Guth, 1942)

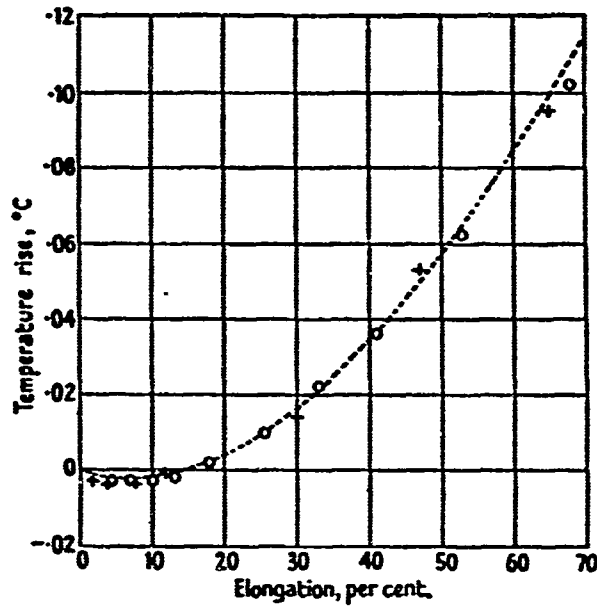


Fig. 21 Temperature rise in adiabatic extension. + Joule's experiments. o James and Guth's experiments. --- James and Guth, Theoretical

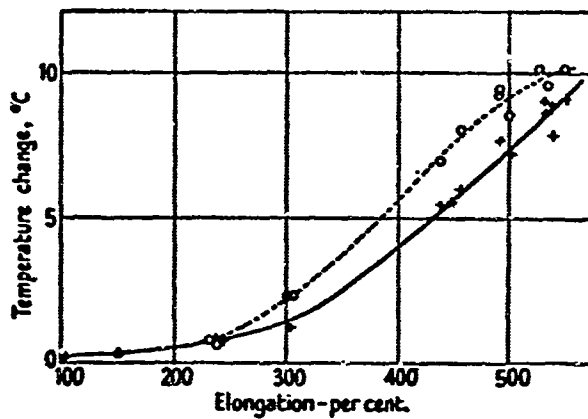


Fig. 22 Temperature change in adiabatic extension (or retraction).  
 ————Extension. ----Retraction.  
 (Dart, Anthony, and Guth, 1942)



Fig. 23 Types of failure of technical rubber under tension. 1. Shear  
 2. Shear and rupture. 3. Rupture.

SECRET  
UNCLASSIFIED

FORM 0 4340

RECEIVED

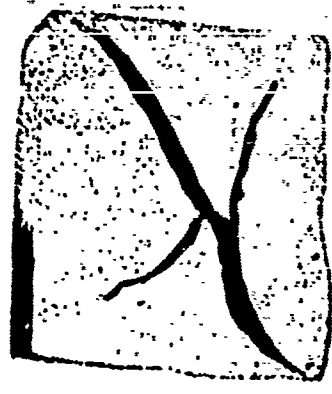


Fig. 24 Failure of rubber sample under compression (chief tear under an angle of  $45^{\circ}$ )

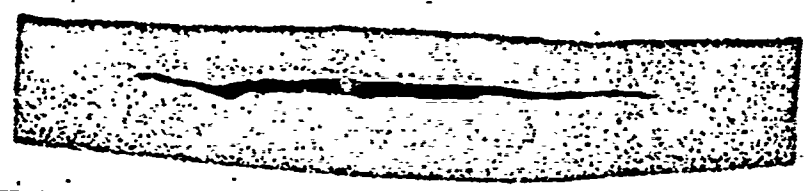


Fig. 25 Failure of rubber sample under compression (tear on the lateral surface of the rubber packing)

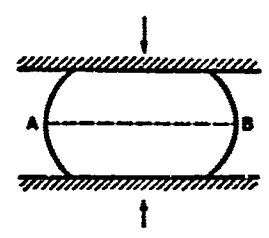


Fig. 26 Schematic deformation of rubber specimen under compression without slipping along the supporting surfaces (formation of "barrel")